46th AIAA Aerospace Sciences Meeting and Exhibit
7 - 10 January 2008, Reno, Nevada

AIAA 2008-787

Mixing Characteristics of Elliptical Jets with Plug

Marco Debiasi[1], Marco Robert Herberg[2], and Her Mann Tsai[3]
Temasek Laboratories, National University of Singapore, Singapore, 117508, Singapore

and

Dimitri Papamoschou[4]
Department of Mechanical and Aerospace Engineering, University of California, Irvine, CA 92697-3975, USA

It is known that elliptical jets entrain surrounding air more effectively than round jets. Past studies also show that convergent-divergent nozzles operated at overexpanded conditions create flow instabilities that enhance the jet mixing. A convergent-divergent passage can be created between an elliptical nozzle and a round plug. The exit-to-throat height of the annular passage is non uniform around the nozzle. The aim of the present study is to investigate the characteristics of this arrangement which is expected to produce vigorous mixing. The mean velocity fields of subsonic-speed jets from such nozzle configuration were surveyed using an array of Pitot probes. Comparisons were made between jets using elliptical nozzles with plug at various pressure and exit-to-throat area ratios and jets from round, convergent nozzles with plug. The results indicate that elliptical nozzles with plug split the flow in two cores. This increases the mixing and promotes faster velocity decay in the plume. The flow instabilities associated to overexpanded conditions in the nozzle also contribute to enhance the mixing.

Nomenclature

A_e	=	nozzle cross-sectional area at exit plane
A_t	=	nozzle cross-sectional area at throat plane
a	=	radius along the major axis of elliptical nozzle
b	=	radius along the minor axis of elliptical nozzle
D	=	equivalent nozzle diameter
IR	=	infra-red signature of jet
IR_{ref}	=	reference infra-red signature of jet
M	=	local Mach number
M_e	=	Mach number at exit of the nozzle
M_i	=	Mach number of the isentropically expanded, pressure-matched jet
NPR	=	nozzle pressure ratio
Q	=	volume flow rate of the jet
$\Delta r_e(\zeta)$	=	gap between nozzle and plug at exit plane
$\Delta r_t(\zeta)$	=	gap between nozzle and plug at throat plane
Re_D	=	Reynolds number based on the equivalent nozzle diameter
T	=	static temperature of the flow
T_0	=	total temperature of the flow
T_∞	=	ambient temperature
T_{ref}	=	reference static temperature

[1] Research Scientist, Temasek Laboratories, National University of Singapore, Singapore, Member AIAA.
[2] Associate Scientist, Temasek Laboratories, National University of Singapore, Singapore.
[3] Senior Research Scientist, Temasek Laboratories, National University of Singapore, Singapore, Member AIAA.
[4] Professor, Department of Mechanical and Aerospace Engineering, University of California, Irvine, California, USA, Associate Fellow AIAA.

U_e = velocity at the exit of the nozzle
U_i = velocity of the isentropically expanded, pressure-matched jet
u = local horizontal component of flow velocity
u_{max} = maximum horizontal component of flow velocity at streamwise location
x = longitudinal coordinate
y = spanwise coordinate
z = vertical coordinate
ζ = azimuthal angle

I. Introduction

ENHANCING the mixing of jets with the surrounding air is crucial to improve the noise and thermal emission of aero engines. The thrust, weight, and complexity penalties introduced by the mixing process must be minimized for practical aircraft applications. This problem has increasing relevance to the exhaust of modern military fighters and unmanned aerial vehicles. A recent review of the state of the art is given by Knowles and Saddington.[1]

Direct mechanical methods, such as lobe mixers[2,3] and vortex generators[4], can cause significant losses that increase with the jet Mach number and can reach as much as 10% in supersonic jets.[5] Non-mechanical means, such as a counter-current shear layer to increase shear[6] or unsteady transverse jets installed at the nozzle exit to destabilize the jet[7] show good mixing. However such fluidic control methods also introduce performance and axial momentum losses and require complex ducts for flow distribution. High-aspect-ratio rectangular nozzles promote very effective mixing of the jet with the ambient air and have been successfully used for reducing the infra-red signature of jet engines. On the other hand, the physical transition from circular to rectangular flow requires additional space and weight, and introduces significant aerodynamic losses. Intermediate shapes between the two simple and asymptotic geometries (round and rectangular), such as elliptic ones, can be alternatives which can offer mixing advantages over the circular case. A considerable amount of experimental investigations is available in the literature that discusses the mixing, entrainment and development of the flow fields of elliptical jets.[8-10] Velocity measurements show that small-aspect-ratio elliptical jets entrain the surrounding fluid more effectively than round jets[8] while introducing small losses. In an elliptical jet the cross-section area and velocity vary nonlinearly within the flow field. Furthermore, the downstream flow field of an elliptical jet exhibits axis switching.

A method for mixing enhancement using axial flow (MEAF) has been recently proposed which does not use mechanical devices to directly disturb the jet. Rather, this is destabilized by the flow separation naturally occurring past a normal shock produced by overexpansion in a convergent–divergent nozzle.[11-17] Separation models by Romine[18] help to identify the range of the suitable nozzle pressure ratios. Expansion and compression waves are created past the main shock which interact with the separated flow and destabilize it, see Fig. 1. The shear layer of the large separation zone is particularly unstable. The flow instabilities grow outside the nozzle and form very large eddies that increase the jet entrainment and reduce the jet velocity. The characteristics of this type of flow from two-dimensional nozzles were studied by using centerline Pitot surveys, laser-induced fluorescence, surveys of the entire velocity field, and flow simulations.[11-17] The results predict small thrust penalty (1-2%) and the technique is characterized by the simplicity of the nozzles.

Adding a round plug to an elliptical nozzle is a mean to create a convergent-divergent annular passage with azimuthally non-uniform exit-to-throat ratio. Overexpanded flow in such annulus is expected to induce MEAF effects that vary around the nozzle. The scope of the current work is a preliminary assessment of the characteristics of the jets issuing from this type of nozzle arrangement. In particular we are interested to explore the effect of non-uniform circumferential separation associated to overexpanded nozzle operation. At the same time we are interested to identify interactions with the typical phenomena observed in elliptical jets. To this aim, the mean velocity fields of subsonic jets were surveyed using an array of Pitot probes. Jets from elliptical nozzles with plug at different exit-to-throat area ratios were compared to the baseline flow from a convergent, round nozzle with plug, a configuration applicable to the exhaust of subsonic jet and turboprop engines. The experimental measurements were used to derive velocity distributions, to quantify the mixing of the plume, and to estimate its temperature distribution.

The following sections describe the nozzle geometries and flow conditions explored, the experimental setup, followed by different type of data analysis and discussion of the corresponding results.

II. Experiments

A. Nozzles

The nozzle configuration and nomenclature used in this study are shown in Fig. 2. The configuration is similar to that used on a previous study of dual-stream, round nozzles with plug.[19] We tested two elliptical nozzles with aspect ratio a/b = 1.25 and 1.5 which have the same exit area of a round nozzle (a/b = 1.00) of diameter D = 31.6mm (1.24in). The nozzles comprise successive segments: an initial convergence to a round section of diameter D, a smooth transition from round to elliptical shape maintaining the same area (for the elliptical nozzles only), and a straight final segment to the nozzle lip. The same plug was used in all the nozzle arrangements which has round sections and bulges slightly before tapering. The nozzles and the plug were created from epoxy resin material using stereolithography rapid-prototyping. A sonic throat is created between the plug bulge and the straight segment of the nozzle before the exit. The overall exit-to-throat area ratio A_e/A_t increases with recessing the plug relative to the nozzle. The symbols in Fig. 2 indicate the position of the plug bulge with respect to the nozzle lip for the exit-to-throat area ratios explored in this study. For the elliptical nozzles, the exit-to-throat area ratio between the nozzle and the plug changes along the azimuthal angle ζ, Fig. 3. This is intended to create a non-uniform MEAF effect when the nozzles are operated at overexpanded conditions. For the nozzle pressure ratios considered in this study, best MEAF results are expected with exit-to-throat area ratio between 1.1 and 1.3 [11], i.e. close to the direction ζ=90° of the ellipse major axis. At ζ=0° the gap Δr_t of the throat of the a/b =1.50 elliptical nozzle is only 0.76mm, almost one tenth of the gap (7.2mm) at ζ=90°. Thus when passing through this nozzle most of the flow would move on the sides of the plug along the major axis of the ellipse.

B. Flow Conditions

Table 1 lists the nomenclature and the flow conditions of the cases surveyed in this study.

The experiments covered jets with nozzle pressure ratios (NPR) equal to 1.2, 1.3, and 1.5, which are representative of subsonic exit conditions for turbine engines. The second and third columns of Table 1 give the Mach number M_i and velocity U_i of the flow isentropically expanded to ambient pressure. At each pressure ratio the jet from the convergent (A_e/A_t = 1.0) passage between the round (a/b = 1.0) nozzle and plug is the baseline against which the flows from the elliptical (a/b = 1.25 and 1.50) nozzle arrangements with A_e/A_t = 1.0, 1.4, and 1.7 are compared. For each value of A_e/A_t we identified two possible regimes based on the nozzle NPR as shown in Ref. 11. These are indicated in Table 1 as 'subsonic' and 'internal shock'. In the subsonic cases the flow in the nozzle is entirely isentropic and the corresponding relations can be used to calculate the nozzle exit conditions. In the internal-shock cases the location of the shock was estimated with a cubic-spline interpolation/extrapolation of the shock position data from Fig. 9 of Ref. 14. Knowing the shock location and the corresponding total-pressure loss, the Mach number M_e and velocity U_e of the pressure-matched flow at the nozzle exit were computed. These and the Reynolds number based on the equivalent nozzle diameter D are listed in the last three columns of Table 1. These values are not given for internal shock at NPR=1.2 and A_e/A_t = 1.0, since the extrapolation procedure to locate the shock in this case was deemed not accurate.

C. Mean Velocity Measurements

The nozzles with plug were attached to the apparatus schematized in Fig. 4. Pressure transducers (Setra Model 208E) connected to the nozzle plenum allow control of the jet total pressure within ±1% of the nominal value.

A Pitot rake, shown in Fig. 5, was used to survey the total pressure in the jet plume. The rake consists of five stainless steel tubes, each 70 mm long, supported by an airfoil-shaped holder. The tubes are mounted 12.5 mm apart and their inner diameter is 1.0 mm. The rake is mounted on a carriage with motorized motion in the x-direction (longitudinal) and in the y- and z-directions (spanwise and vertical directions). The first from the top probe is the reference probe, and it was initially positioned at the tip of the plug. The five probes of the rake are individually connected to five pressure transducers (Setra Model 208E). The transducers are mounted close to the traverse assembly in order to minimize the length of the tubing between each probe and the corresponding transducer. The jet Mach number and velocity were computed from the Pitot pressure by assuming constant total temperature and uniform static pressure equal to the ambient values.

The control of the three-axis carriage allowed incremental-step motion in each direction. 1000 samples from each probe were acquired at each new position with a National Instrument 6014 board installed on a Dell Optilex GX270 personal computer.

Streamwise velocity profiles were obtained in the x-y (ellipse's major axis) and x-z (minor axis) planes. For each flow 26 uniformly spaced x-locations were surveyed downstream of the plug tip, with x/D spanning a distance from

0 to about 12. For each axial location 60 measurements separated by 2.08 mm, i.e. one fifth of the probe spacing, were taken in the y and z directions. Cross-sectional surveys were performed at axial distances of x/D = 1, 2, and 4 from the plug tip. The rectangular sampling grids are centered with the jet axis and have points separated by 2.08mm. A large enough number of points in the y and in the z direction was used for each grid to ensure this covered the edges of the plume at each downstream location.

III. Results and Discussion

A. Velocity Fields

Figures 6-10 present some of the velocity isocontours we derived from the Pitot measurements of flows at NPR=1.2. The dimensions are normalized by the equivalent nozzle diameter D, whereas at each pressure ratio the velocity is normalized by the corresponding value of U_i.[19]

Figure 6 presents the longitudinal velocity isocontours of the baseline NPR=1.2 jet. At this pressure the flow inside the converging annulus between the nozzle and the plug is subsonic and should not have any shock. This jet exhibits a high-speed core ($u/U_i > 0.9$) extending about two diameters past the plug tip.

For the same conditions Figs. 7 and 8 present the longitudinal and the cross-sectional isocontours of the jets from the a/b=1.25 elliptical nozzles. This nozzle and plug combined at A_e/A_t = 1.0 split the jet in two distinct and diametrically opposite cores, Fig. 7. This effect is clearly visible in the cross-sectional contour at x/D = 1.0, Fig. 7c. Further downstream the cores decay and eventually merge, Figs. 7d and 7e. The cross-sectional contours reveal also an overall rotation of the plume. We attribute this to unbalanced flow conditions inside the nozzle. As a result the jet, initially larger in the direction y of the ellipse major axis, does not grow much in this plane whereas the opposite occurs in the direction z of the minor-axis, Figs. 7a and 7b. This is accompanied by a slight contraction (10%) of the core region compared to the baseline case. Increasing the nozzle area ratio to A_e/A_t = 1.7 is expected to introduce a shock system in the convergent-divergent annulus between the nozzle and the plug. The flow produced by this configuration, Fig. 8, exhibits the same fundamental characteristics of the previous case: the flow splits in two cores and there is an overall downstream rotation of the plume. However, the decay of the cores and the downstream spreading of the plume in the direction of its local (rotating) major axis are significantly higher than in the convergent case. We attribute this to the mixing enhancement by the separated, overexpanded flow in the annular passage between the nozzle and the plug.

Using the more elliptical a/b=1.50 nozzle accentuates the splitting of the jet in two distinct cores on opposite sides of the plug, Figs. 9 and 10. As a result, the jet flattens more. The longitudinal contour in the x-z (minor axis) plane passes between the cores and does not capture them, Fig. 9b and 10b. In the A_e/A_t = 1.0 case there is minimal rotation of the plume which grows steadily in the direction y of the major axis of the nozzle. The A_e/A_t = 1.7 configuration rotates the plume a little more but much less than the corresponding case with a/b = 1.25.

For brevity, we do not present the velocity isocontours of the elliptical nozzles and plug at A_e/A_t = 1.4 as these are similar to those presented above for A_e/A_t = 1.0 and 1.7.

Similar results were also observed at higher NPR values and lead to the following general comments. The main effect of elliptical nozzles with plug is the splitting of the jet into two cores. The phenomenon is more pronounced with the more elliptical a/b = 1.50 nozzle. The spreading of the plume and the velocity decay both increase with A_e/A_t, i.e. with the mixing enhancement by the overexpanded flow. This appears also to increase the downstream rotation of the plume, possibly a result of asymmetric flow separation in the passage between the nozzle and the plug at overexpanded conditions. It should be noticed that supersonic nozzle flow is known to separate asymmetrically even in symmetric nozzles[13-17]. The plumes from arrangements using the more elliptical nozzle appear less influenced by the effects of overexpansion and exhibit minimal downstream rotation.

B. Maximum Velocity

Figures 11 and 12 present the axial distribution of the local maximum velocity u_{max}. This quantity is often used as a metric to assess various jet characteristics including mixing which typically decreases the jet velocity. At each pressure ratio we normalized u_{max} by the corresponding value of U_i. The baseline jets are axisymmetric and the value of u_{max} at each streamwise location can be obtained from velocity measurements in the longitudinal x-z plane. This can not be done for elliptical-nozzle cases since the longitudinal plane containing u_{max} rotates as discussed in the previous section. Proper capturing of u_{max} would require cross-sectional measurements at each streamwise location, a prohibitively tedious and expensive process. Therefore we present the maximum values from the velocity measurements in the longitudinal x-y plane along the major axis of the ellipse. Near the plug tip this plane is close to u_{max}, Figs. 7-10c. Further downstream (x/D > 4) the cores merge and the jet profiles tend to become more axisymmetric, Figs. 7-10e, so the x-y plane should be able to capture the local value of u_{max}. However, for the

elliptical cases Figs. 11 and 12 also present as solid symbols the true values of u_{max} from the cross-sectional velocity measurements at x/D = 1, 2, and 4. These values can be used to assess the discrepancy of the corresponding distributions of u_{max} from the x-y plane.

The figures indicate that, even for the baseline cases, the velocity decay starts immediately at the plug tip. We believe this is an effect of the contoured plug. The maximum-velocity distribution of the baseline cases is substantially independent of the nozzle pressure ratio. The maximum-velocity distribution of the flows from the a/b = 1.25 nozzle with A_e/A_t = 1.0 are very similar to the corresponding baseline cases, Fig. 11. Arrangements with larger A_e/A_t briskly decrease the jet velocity. The configuration with A_e/A_t =1.7 is particularly effective as it reduces the maximum velocity by about 40% within a distance of 2 diameters from the plug tip. Increasing the values of NPR does not appear to affect much the performance of this configuration.

The maximum-velocity of the flows from the a/b = 1.50 nozzles with A_e/A_t = 1.0 decays faster than the corresponding baselines at all NPRs, see Fig. 12. While the velocity decay is not as high as with A_e/A_t = 1.4 and 1.7, it is obtained by using a configuration that arguably suffers smaller aerodynamic losses. The most effective configuration is with A_e/A_t = 1.7 for which the maximum-velocity distribution is very similar to the corresponding a/b = 1.25 cases. Thus it appears that using elliptical nozzles with plug at A_e/A_t = 1.7 provides strong velocity reduction independent of the NPR and a/b values explored in this study.

C. Mixing Characteristics

The effect of mixing enhancement can be better understood by analyzing the axial distribution of the jet volume flow rate Q. The procedure to obtain this quantity is similar to that outlined by Papamoschou et al.[13] The values presented in Figs. 13 and 14 are normalized by the volume flow rate Q_i of the nozzle flow expanded isentropically to ambient pressure. Results are presented for the elliptical nozzles at x/D = 1, 2, and 4 where we obtained cross-sectional measurements. This scarcity of data limits our discussion to the analysis of overall trends. More data based on the longitudinal velocity profiles are available for the axisymmetric baseline jets. In the range x/D = 1-4 these jets grow almost linearly. Replacing the round nozzle with the a/b = 1.25 elliptical nozzle, Fig. 13, increases the volume flow rate but this advantage diminishes with increasing NPR. Using larger values of the exit-to-throat area ratio further benefits the jet mixing. At a distance of 4 diameters from the plug tip the configurations with A_e/A_t = 1.7 appear capable of doubling the volume flow rate of the corresponding baselines. The more elliptical a/b = 1.50 nozzle produces overall similar trends, Fig. 14. However in this case the mixing benefits decrease with NPR for all values of A_e/A_t.

A pertinent application of the mixing techniques discussed in this work is increasing the mixing and reducing the infra-red signature of turbine aero engines. As a study case we considered the exhaust of a typical turboprop engine. The flow conditions of the exhaust of such an engine have been derived by analyzing the corresponding Brayton-Joule cycle. By matching the compressor pressure ratio, the turbine inlet temperature, the shaft power, and other relevant parameters[20] we estimated a total temperature of about 750K and a pressure ratio of about 1.2 for the nozzle flow, one of the conditions covered in this work.

With the assumption that the radial components of the jet velocity are small compared to axial ones, the gradients are bigger in the radial than in the axial direction, and the Prandtl number for air is close to unity, we estimated the plume temperature distribution of the NPR=1.2 jets by using the Crocco-Busemann relation. We imposed the boundary conditions T_0 = 750K for $u = U_i$ at the nozzle exit and $T_0 = T_\infty$ for u = 0 far from the jet. The plume static temperature distribution was then obtained from the total temperature and the Mach number distributions. These are shown in Figs. 15 and 16 and effectively consist of rescaling the corresponding velocity contours. For the elliptical-nozzle cases we present only the data in the x-y plane where the higher temperatures are found.

By using the procedure above we estimated the maximum temperature of the baseline jet to be 700K in the annular core region close to the plug, Fig. 15. The a/b=1.25 elliptical nozzle with plug at A_e/A_t =1.0 produces a similar temperature distribution, Fig. 16a. Increasing A_e/A_t to 1.7 produces a substantial thermal benefit, Fig. 16b. The maximum temperature close to the plug is reduced by about 50K. This translates in a drop of the peak infra-red signature of about 40% according to the relationship for plume infra-red signature derived by Banken et al.[21]

$$IR = IR_{ref}\left(\frac{T}{T_{ref}}\right)^{m} \tag{1}$$

where the reference temperature T_{ref} corresponds to the maximum temperature of the baseline and the exponent m varies linearly between 9 ($T \approx 350$ K) and 6 ($T \approx 1000$ K). Further downstream the temperature drop with respect to the baseline is about 100K and the size of the radiating plume is also reduced which is considered crucial to improve the thermal signature of a jet.[1] The combination of these factors is expected to produce an overall thermal reduction in excess of 40%. The a/b=1.50 elliptical nozzle with plug at A_e/A_t =1.0 produces a different temperature distribution than the a/b=1.25 nozzle, but with similar maximum values, Fig. 16c. The thermal benefit of this nozzle used at A_e/A_t =1.7, Fig. 16d, is similar to that discussed above for the corresponding a/b=1.25 case.

It should be emphasized that the values above represent an estimate of the plume temperature distribution. Specific temperature measurements using hot-jets need to be performed to precisely assess the thermal benefit of any mixing technology.

IV. Conclusions

The mixing characteristics of subsonic jets issuing from elliptical nozzles with a central round plug have been investigated through mean velocity measurements of the flow fields. The experiments covered jets with nozzle pressure ratios representative of subsonic exit conditions for turbine engines. The main effect of elliptical nozzles with plug is the splitting of the flow in two distinct cores on opposite sides of the plug. This promotes the mixing of the jet with ambient air. The mixing is also enhanced by the effects of flow separation at overexpanded conditions. This phenomenon is mostly controlled by the exit-to-throat area ratio A_e/A_t of the annular passage between the nozzle and the plug. The influence of the nozzle pressure ratio and of the nozzle eccentricity are minor. The jet mixing increases with A_e/A_t. At a downstream distance from the plug tip of four diameters the elliptical nozzle and plug configurations with A_e/A_t = 1.7 can double the volume flow rate compared to the baseline flow from a round, convergent nozzle with plug. The stronger mixing decreases the jet velocity. 40% reductions of the maximum jet velocity have been observed within a distance of 2 diameters from the plug tip. The jet plume rotates as it flows downstream. This rotation also appears to increase with A_e/A_t, possibly as a result of asymmetric flow separation with overexpanded conditions in the annular passage between the nozzle and the plug. An estimate of the plume temperature based on the Crocco-Busemann relation was performed. This analysis indicates that the elliptical nozzles with plug can reduce the hottest spots in the jet plume by 50 K compared to the baseline case. This translates into a 40% reduction of the peak infra-red signature.

This work will be complemented by an analogous study on the mixing enhancement of round nozzles with plug operated at overexpanded conditions. Additional work is required to better understand the physics of flow separation in asymmetric, convergent-divergent nozzles. Similar to previous studies on symmetric configurations, these will include experiments and computations on two-dimensional nozzles. The results will be relevant to the flow separation occurring in the annular passage between the nozzle and the plug.

Acknowledgments

We are grateful to Mr. Lim Kim Seng for his assistance with constructing the jet and running the experiments.

References

1. Knowles, K. and Saddington, A. J., "A review of jet mixing enhancement for aircraft propulsion applications," Proceedings of the Institution of Mechanical Engineers, Part G: *Journal of Aerospace Engineering*, Vol. 220, No. 2, 2006, pp. 103-127.
2. Westley, R., and Lilley, G. M., "An Investigation of the Noise Field from a Small Jet and Methods for Its Reduction," College of Aeronautics, Report 53, Cranfield Univ., England, UK, 1952.
3. Zaman, K. B. M. Q, Wang, F. Y., and Georgiadis, N. J., "Noise, Turbulence, and Thrust of Subsonic Freejets from Lobed Nozzles," *AIAA Journal*, Vol. 41, No.3, pp. 398-407.
4. Zaman, K. B. M. Q., Reeder, M. F., and Samimy, M., "Control of an Axisymmetic Jet Using Vortex Generators," *Physics of Fluids*, Vol. 6, No. 2, pp. 778-796.
5. Zaman, K. B. M. Q., "Jet Spreading Increase by Passive Control and Associated Performance Penalty," AIAA Paper 99-3505.
6. Strykowksi, P. J., Krothapalli, A., and Jendoubi, S., " The Effect of Counterflow on the Development of Compressible Shear Layers," *Journal of Fluid Mechanics*, Vol. 308, pp. 63-96.
7. Raman, G., "Using Controlled Unsteady Fluid Mass Addition to Enhance Jet Mixing," *AIAA Journal*, Vol. 35, No. 4, pp. 647-656.
8. Ho. C. M. and Gutmark. E., "Vortex induction and mass entrainment in a small aspect ratio elliptical jet," *Journal of Fluid Mechanics*, Vol. 179, pp. 383-405.
9. Husain. H. S. and Hussain. F., "Elliptical jets. Part 3: Dynamics of preferred mode coherent structure," *Journal of Fluid Mechanics*, Vol. 248, pp. 315-361.
10. Hussain. F and Husain. H.S, "Elliptical jets. Part 1: Characteristics of unexcited and excited jets," *Journal of Fluid Mechanics*, Vol. 208, pp. 257-320.
11. Papamoschou, D., "Mixing Enhancement Using Axial Flow," AIAA Paper 2000-0093.
12. Zaman, K. B. M. Q, and Papamoschou, D., "Study of Mixing Enhancement Observed with a Co-Annular Nozzle Configuration, " AIAA Paper 2000-0094.
13. Papamoschou, D, Dixon, T. D., and Nishi, K. A., "Mean Flow of Multistream Rectangular Jets under Normal and Mixing Enhancement Conditions," AIAA Paper 2004-0919.
14. Papamoschou, D. and Zill, A., "Fundamental Investigation of Supersonic Nozzle Flow Separation," AIAA Paper 2004-1111.
15. Papamoschou, D. and Johnson, A., "Unsteady Phenomena in Supersonic Nozzle Flow Separation," AIAA Paper 2006-3360.
16. Xiao, Q., Tsai, H. M., and Papamoschou, D., "Numerical Investigation of Supersonic Nozzle Flow Separation," *AIAA Journal*, Vol. 45, No.3 pp. 532-541.
17. Xiao, Q., Tsai, H. M., and Papamoschou, D., "Numerical Study of Jet Plume Instability from an Overexpanded Nozzle," AIAA Paper 2007-1319.
18. Romine, G. L., "Nozzle Flow Separation," *AIAA Journal*, Vol. 36, No. 9, pp. 1618-1625.
19. Debiasi, M., Dhanabalan, S. S., Tsai, H. M., and Papamoschou, D., "Mixing Enhancement of High-Bypass Turbofan Exhausts via Contouring of Fan Nozzle", AIAA Paper 2007-4497.
20. Hill, P. and Peterson, C., *Mechanics and Thermodynamics of Propulsion*, 2nd ed., Addison Wesley, Reading, Massachusetts, 1992.
21. Banken, G. J., Cornette, W. M., and Gleason, K. M., "Investigation of infrared characteristics of three generic nozzle concepts," AIAA-80-1160.

Table 1 Nomenclature and flow conditions

NPR	M_i	U_i m/s	a/b	$\frac{A_e}{A_t}$	*Flow regime*	M_e	U_e m/s	Re_D x10^5
1.2	0.52	176	1.00, 1.25, 1.50	1.0	subsonic	0.52	176	3.74
1.2	0.52	176	1.25, 1.50	1.4	internal shock	0.51	173	3.68
1.2	0.52	176	1.25, 1.50	1.7	internal shock	-	-	-
1.3	0.62	210	1.00, 1.25, 1.50	1.0	subsonic	0.62	210	4.57
1.3	0.62	210	1.25, 1.50	1.4	internal shock	0.58	197	4.25
1.3	0.62	210	1.25, 1.50	1.7	internal shock	0.61	205	4.44
1.5	0.78	258	1.00, 1.25, 1.50	1.0	subsonic	0.78	258	5.85
1.5	0.78	258	1.25, 1.50	1.4	internal shock	0.71	235	5.22
1.5	0.78	258	1.25, 1.50	1.7	internal shock	0.73	241	5.38

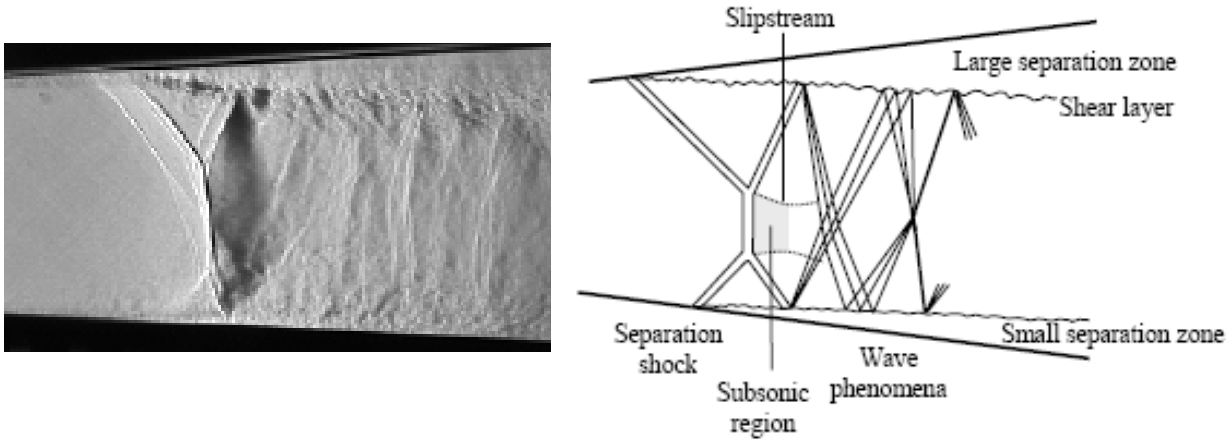

Figure 1. Supersonic nozzle flow separation: spark schlieren image (left); schematic of principal phenomena (right) [from Ref. 15].

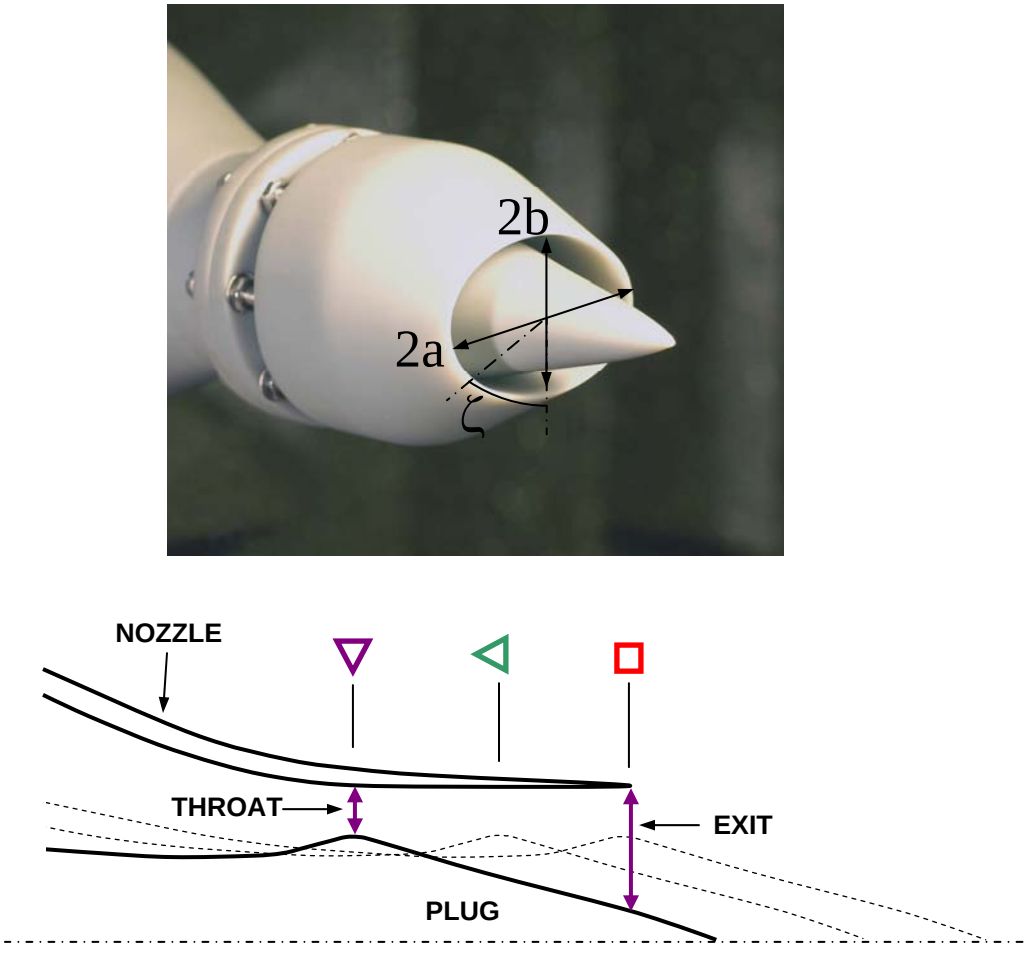

Figure 2. Picture and longitudinal section of the elliptical nozzle with plug. The symbols indicate the position of the plug bulge at: □ A_e/A_t = 1.0 ; ◁ A_e/A_t = 1.4 ; ▽ A_e/A_t = 1.7.

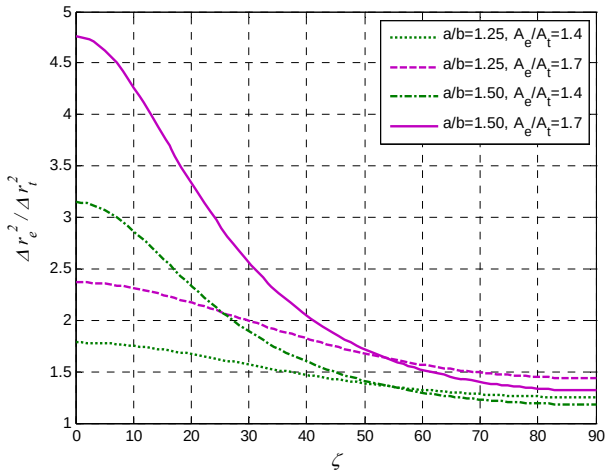

Figure 3. Azimuthal variation of the exit-to-throat area ratio for elliptical nozzles with round plug.

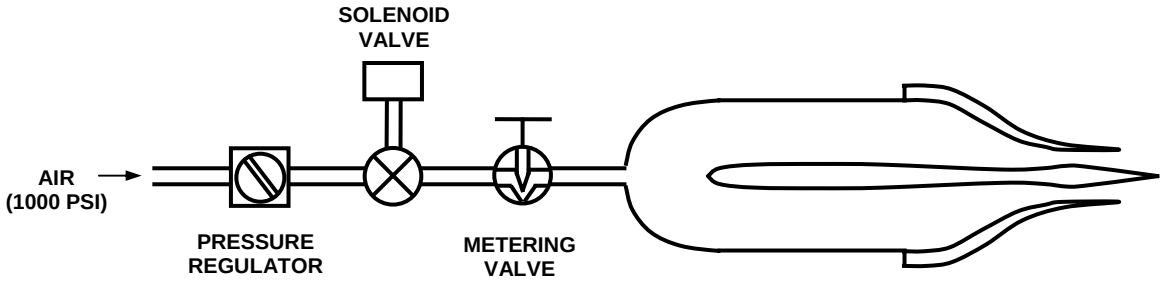

Figure 4. Schematics of the jet facility.

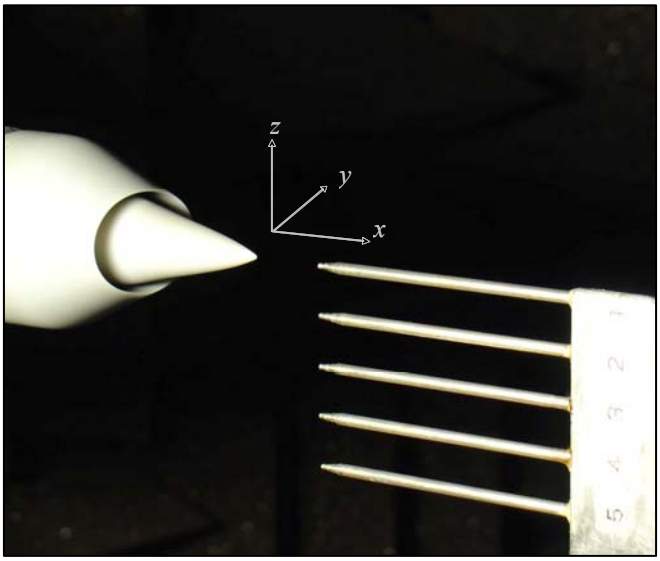

Figure 5. Coordinate system and Pitot rake for mean velocity measurements.

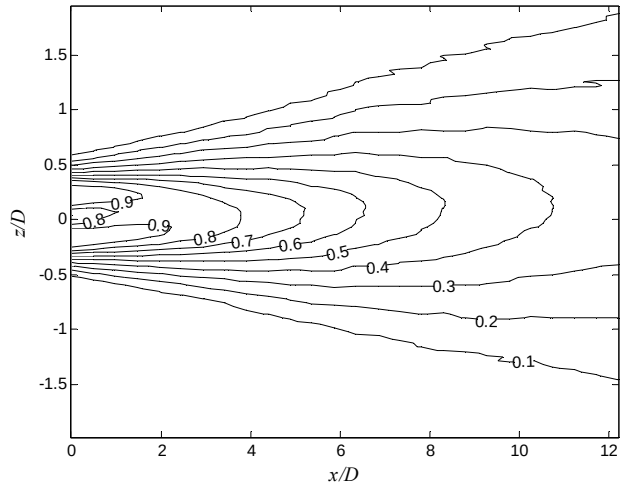

Figure 6. Normalized velocity isocontours of jet from baseline, round nozzle with NPR=1.2.

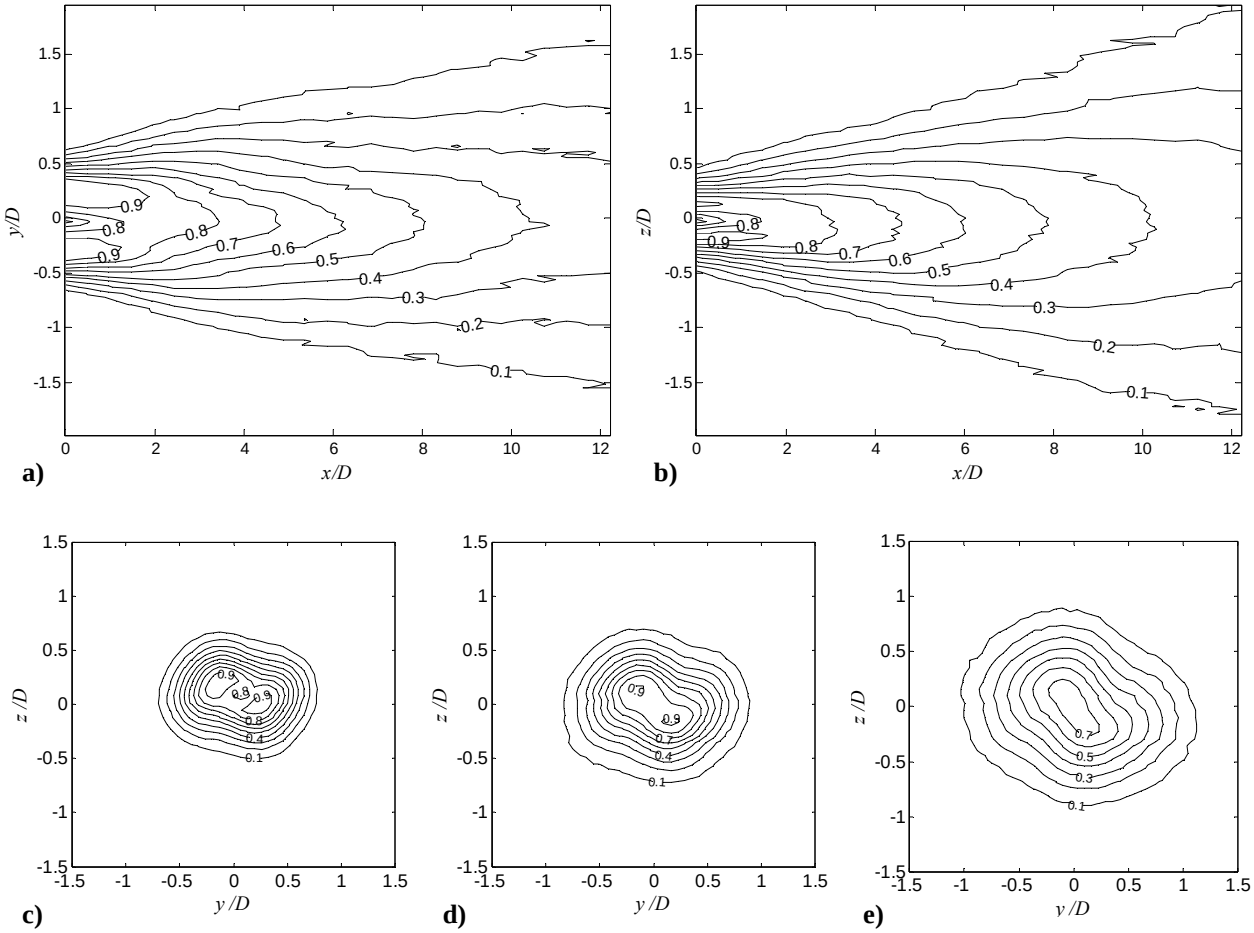

Figure 7. Normalized velocity isocontours of jet from elliptical nozzle with *a*/*b*=1.25, NPR=1.2, and A_e/A_t=1.0. Longitudinal planes along the ellipse: a) major axis; b) minor axis; cross-sectional planes at: c) *x*/*D* = 1; d) *x*/*D* = 2; e) *x*/*D* = 4 .

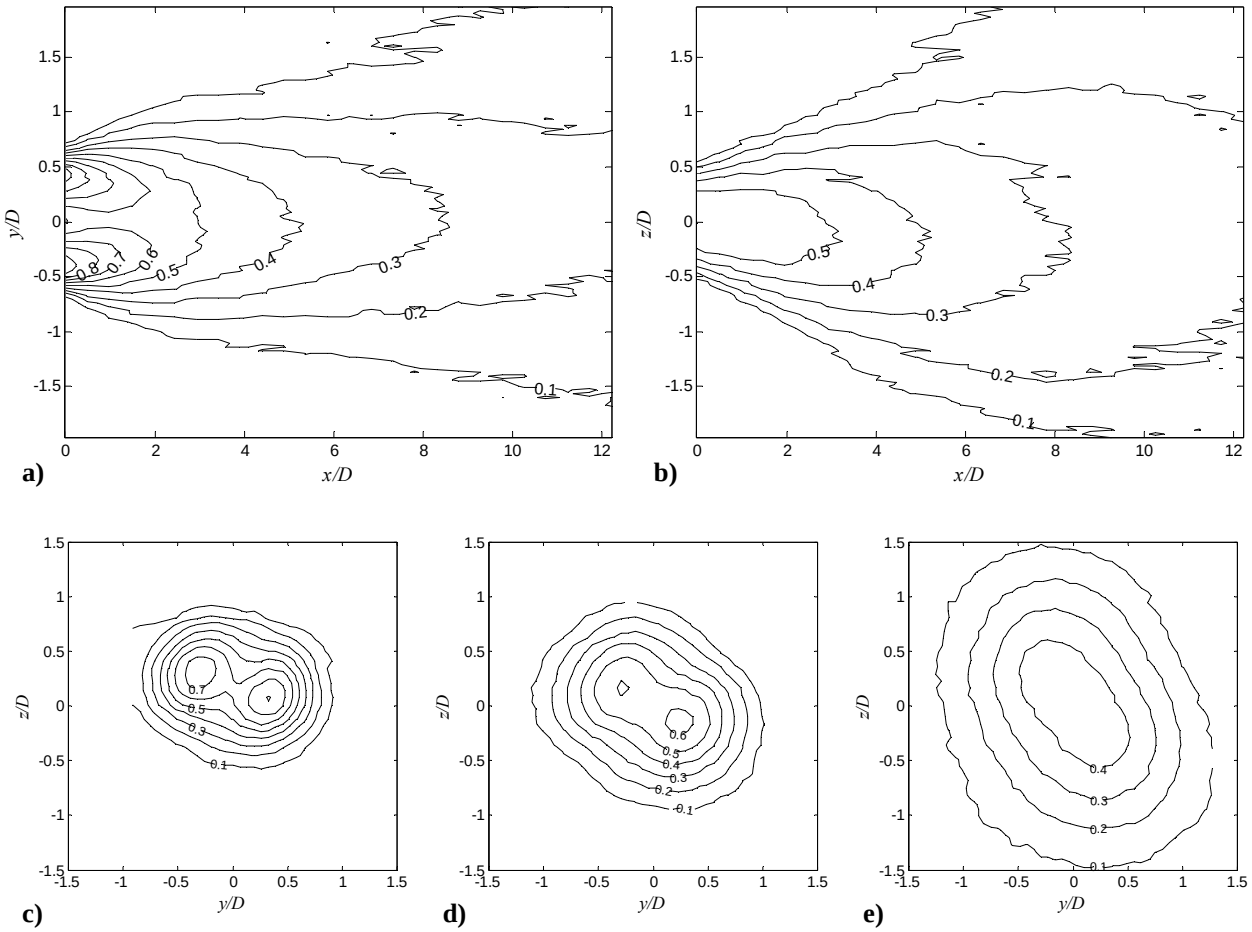

Figure 8. Normalized velocity isocontours of jet from elliptical nozzle with *a*/*b*=1.25, NPR=1.2, and A_e/A_t=1.7. Longitudinal planes along the ellipse: a) major axis; b) minor axis; cross-sectional planes at: c) *x*/*D* = 1; d) *x*/*D* = 2; e) *x*/*D* = 4 .

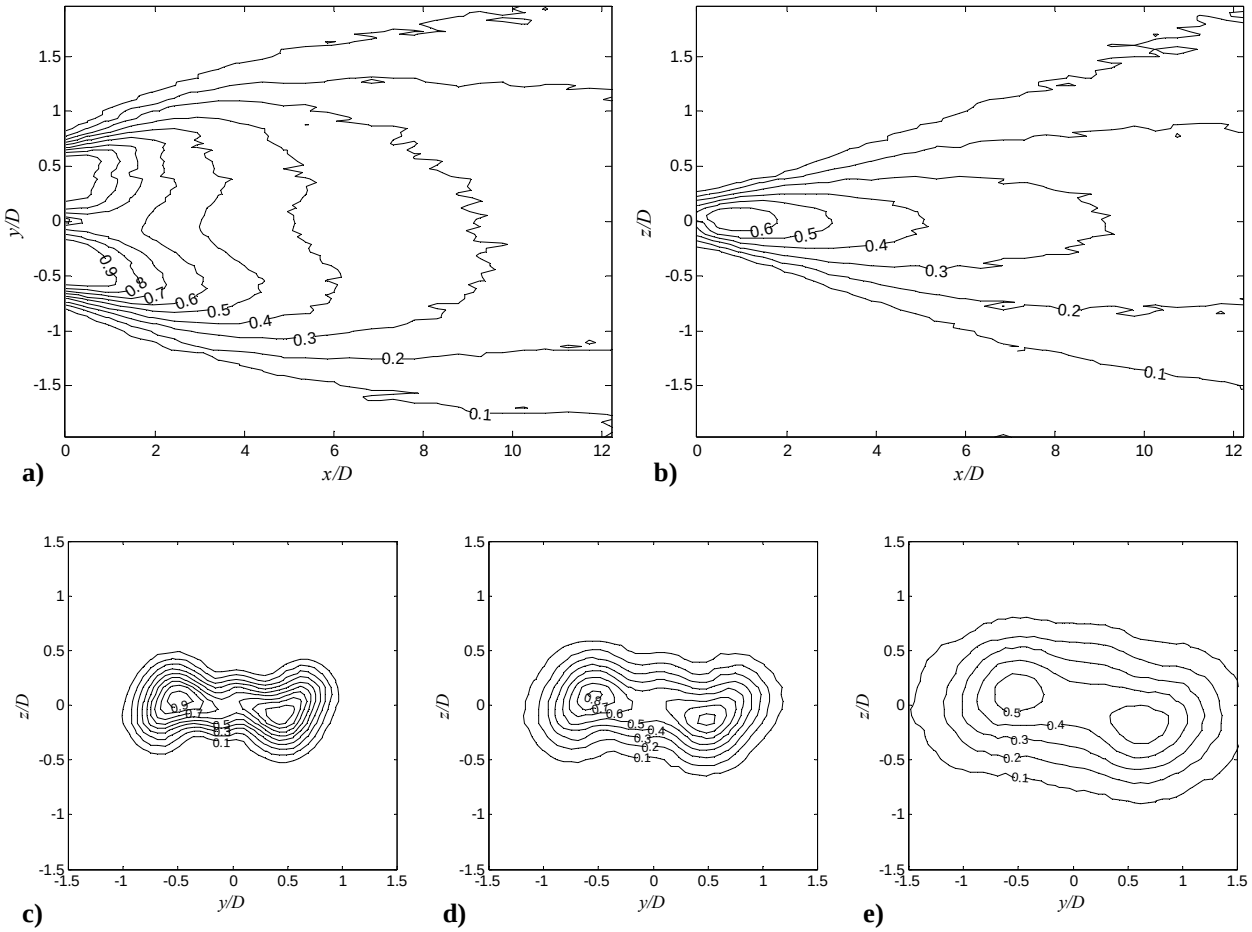

Figure 9. Normalized velocity isocontours of jet from elliptical nozzle with *a*/*b*=1.50, NPR=1.2, and A_e/A_t=1.0. Longitudinal planes along the ellipse: a) major axis; b) minor axis; cross-sectional planes at: c) *x*/*D* = 1; d) *x*/*D* = 2; e) *x*/*D* = 4 .

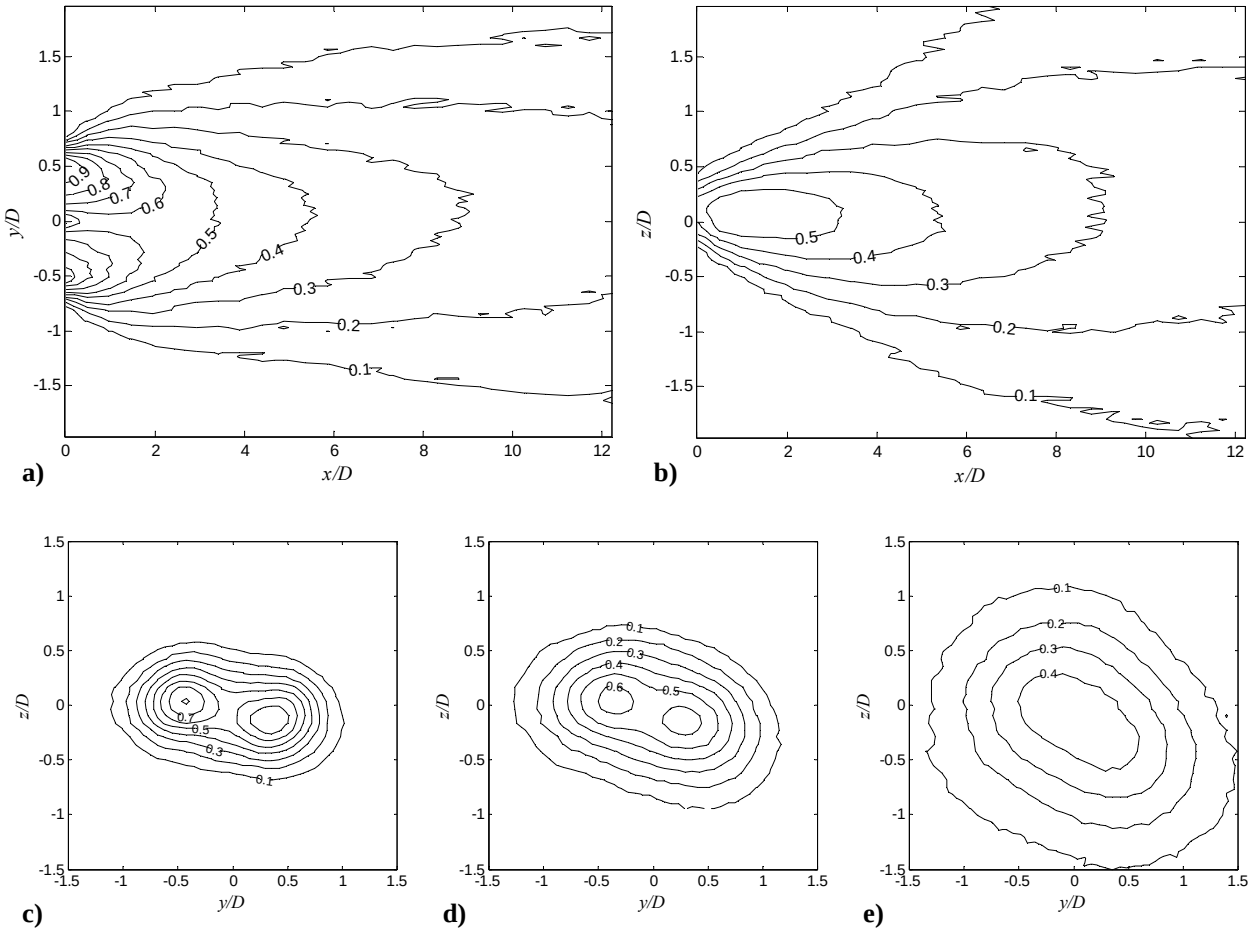

Figure 10. Normalized velocity isocontours of jet from elliptical nozzle with a/b=1.50, NPR=1.2, and A_e/A_t=1.7. Longitudinal planes along the ellipse: a) major axis; b) minor axis; cross-sectional planes at: c) x/D = 1; d) x/D = 2; e) x/D = 4 .

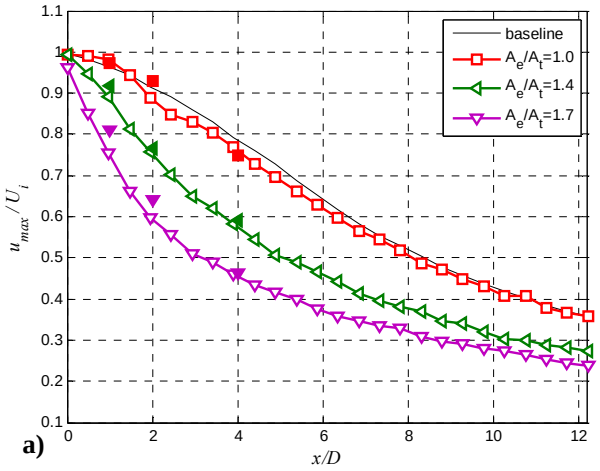

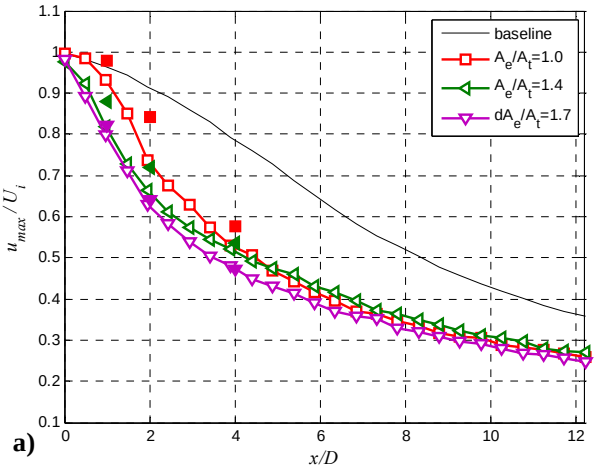

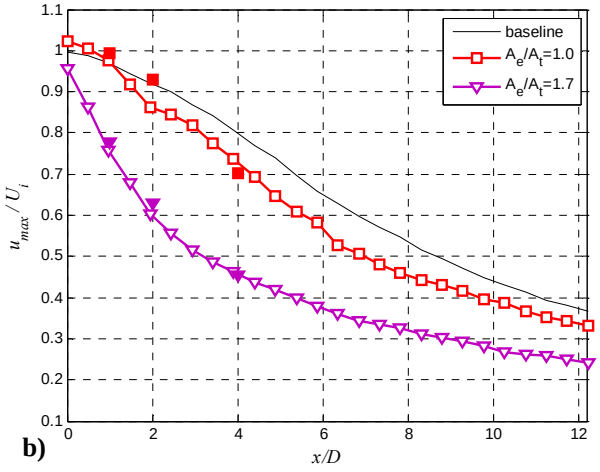

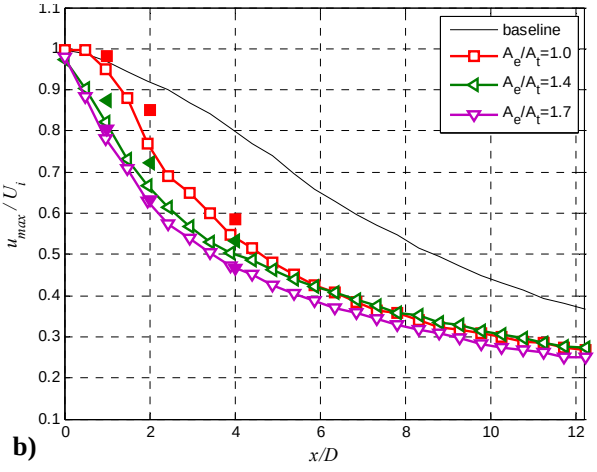

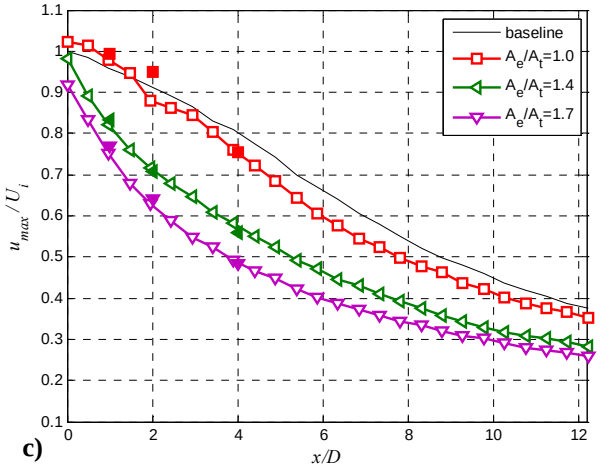

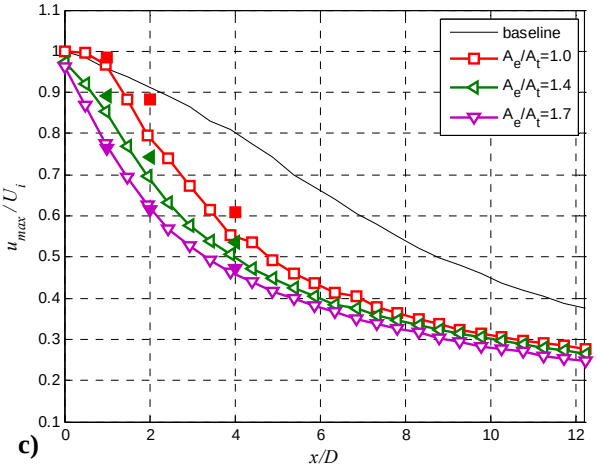

Figure 11. Distribution of normalized local maximum velocity for jets from *a*/*b*=1.25 elliptical nozzles at: a) NPR=1.2; b) NPR=1.3; c) NPR=1.5 . The true values of u_{max} from cross-sectional measurements at *x*/*D* = 1, 2, and 4 are indicated with: ■ A_e/A_t=1.0; ◀ A_e/A_t=1.4; ▼ A_e/A_t=1.7 .

Figure 12. Distribution of normalized local maximum velocity for jets from *a*/*b*=1.50 elliptical nozzles at: a) NPR=1.2; b) NPR=1.3; c) NPR=1.5 . The true values of u_{max} from cross-sectional measurements at *x*/*D* = 1, 2, and 4 are indicated with: ■ A_e/A_t=1.0; ◀ A_e/A_t=1.4; ▼ A_e/A_t=1.7 .

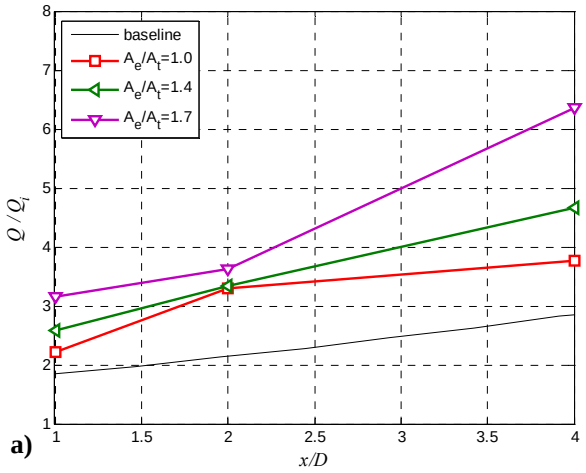

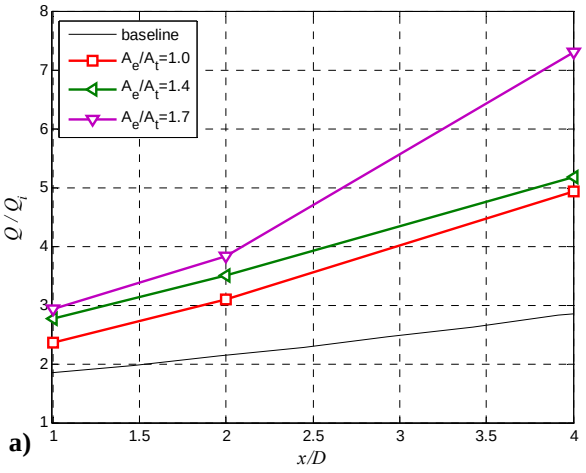

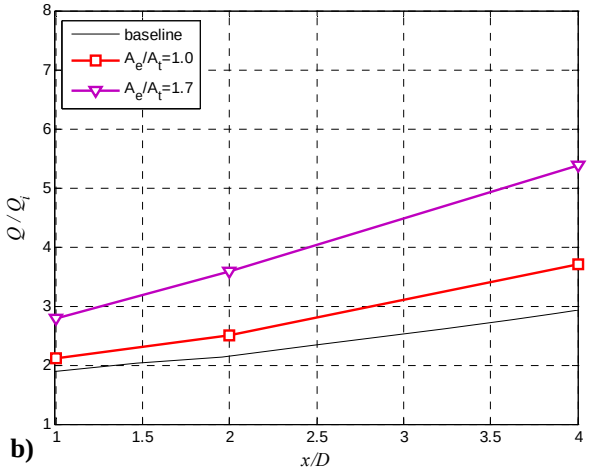

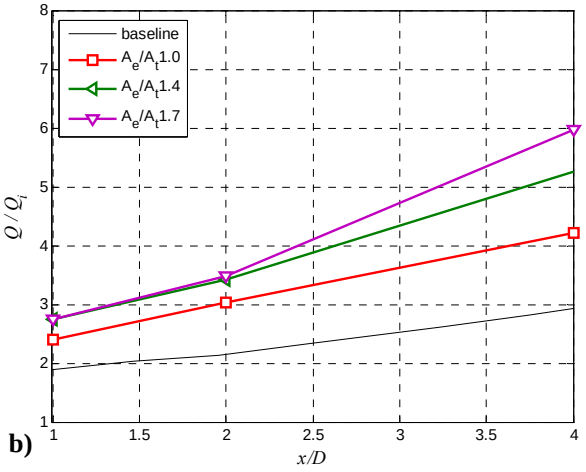

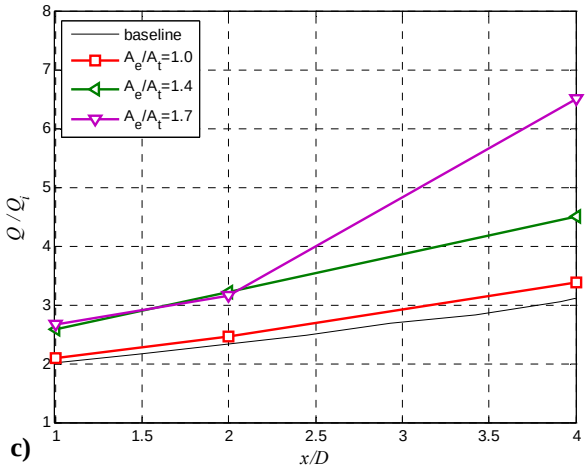

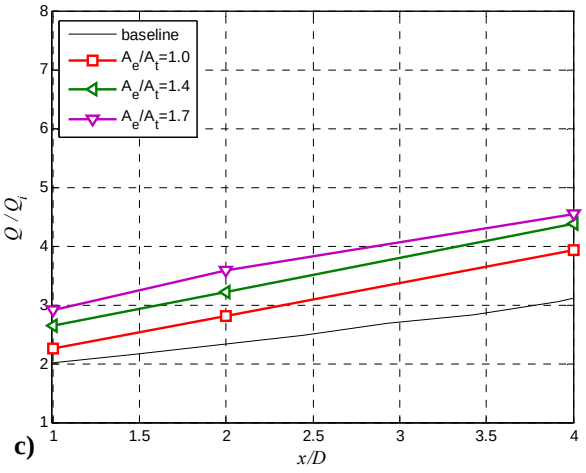

Figure 13. Distribution of normalized volume flow rate of jets from *a*/*b*=1.25 elliptical nozzles at: a) NPR=1.2; b) NPR=1.3; c) NPR=1.5 .

Figure 14. Distribution of normalized volume flow rate of jets from *a*/*b*=1.50 elliptical nozzles at: a) NPR=1.2; b) NPR=1.3; c) NPR=1.5 .

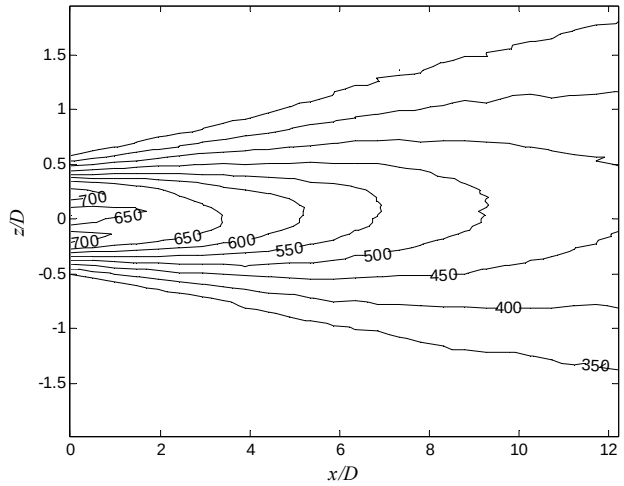

Figure 15. Static temperature from Crocco-Busemann relation of jet from baseline, round nozzle with NPR=1.2.

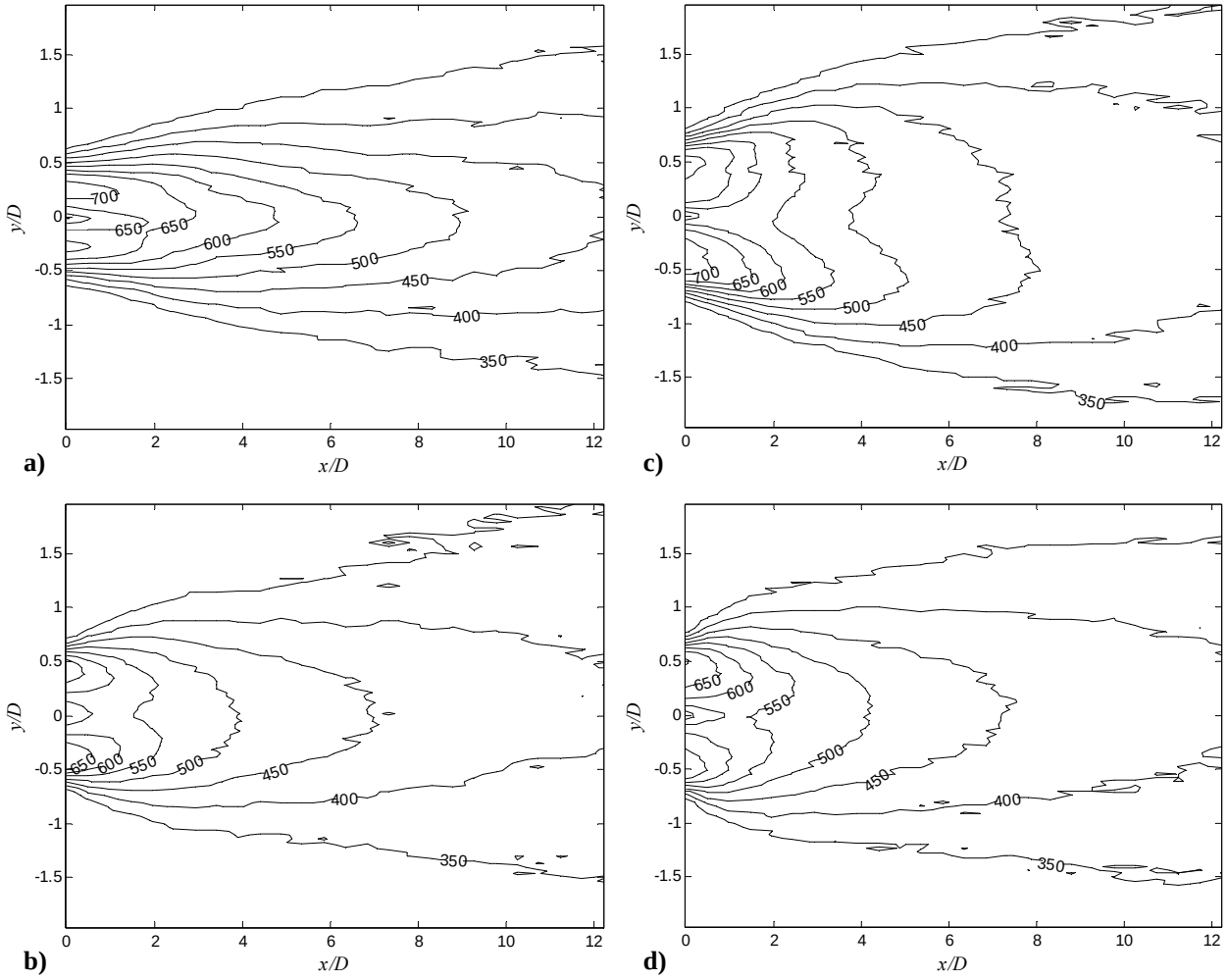

Figure 16. Static temperature from Crocco-Busemann relation of jets from elliptical nozzles with NPR=1.2: a) a/b=1.25, A_e/A_t=1.0; b) a/b=1.25, A_e/A_t=1.7; c) a/b=1.50, A_e/A_t =1.0; d) a/b=1.50, A_e/A_t =1.7.